

1 **The response of diazotrophs to nutrient amendment in the**  
2 **South China Sea and western North Pacific**

3

4 Zuo Zhu Wen<sup>1,2</sup>, Thomas J. Browning<sup>2</sup>, Rongbo Dai<sup>1</sup>, Wenwei Wu<sup>1</sup>, Weiying Li<sup>1,a</sup>,  
5 Xiaohua Hu<sup>1</sup>, Wenfang Lin<sup>1</sup>, Lifang Wang<sup>1</sup>, Xin Liu<sup>1</sup>, Zhimian Cao<sup>1</sup>, Haizheng Hong<sup>1</sup>,  
6 and Dalin Shi<sup>1</sup>

7

8 <sup>1</sup>State Key Laboratory of Marine Environmental Science, Xiamen University, Xiamen,  
9 Fujian, PR China

10 <sup>2</sup>Marine Biogeochemistry Division, GEOMAR Helmholtz Centre for Ocean Research  
11 Kiel, Germany

12

13 *Correspondence to:* Dalin Shi (dshi@xmu.edu.cn) and Haizheng Hong  
14 (honghz@xmu.edu.cn)

15

16 a. Present address: Key Laboratory of Marine Ecosystem Dynamics, Second Institute of  
17 Oceanography, Ministry of Natural Resources, Hangzhou, Zhejiang, PR China

18 **Abstract.** The availability of iron (Fe) and phosphorus (P) have been shown to be key  
 19 factors regulating rates of nitrogen fixation in the western Subtropical Pacific. However,  
 20 their relative importance at finer spatial scales between the northern South China Sea  
 21 (NSCS) and the western boundary of the North Pacific is poorly constrained.  
 22 Furthermore, nutrient limitation of specific diazotroph types has not yet been assessed.  
 23 Here we investigated these unknowns by carrying out measurements of (i) finer scale  
 24 spatial variabilities in N<sub>2</sub> fixation rates and diazotroph *nifH* gene abundances throughout  
 25 these regions, and (ii) conducting eight additional Fe and phosphate addition bioassay  
 26 experiments where both changes in N<sub>2</sub> fixation rates and the *nifH* gene abundances of  
 27 specific diazotrophs were measured. Overall, nitrogen fixation rates and *nifH* gene  
 28 abundances were lower in the NSCS than around the Luzon Strait and the western North  
 29 Pacific. The nutrient addition bioassay experiments demonstrated that N<sub>2</sub> fixation rates in  
 30 the central NSCS were co-limited by Fe and P, whereas in the western boundary of the  
 31 North Pacific they were P-limited. Changes in the abundances of *nifH* in response to  
 32 nutrient addition varied in how well they correlated with changes in N<sub>2</sub> fixation rates, and  
 33 in 6 out of 8 experiments the largest responses in *nifH* gene abundances were dominated  
 34 by either *Trichodesmium* or UCYN-B. In general, nutrient addition had a relatively  
 35 restricted impact on the composition of the six phylotypes that we surveyed apart from on  
 36 UCYN-B. This unicellular cyanobacterium group showed increased contribution to the  
 37 total *nifH* gene abundance following P addition at sites where N<sub>2</sub> fixation rates were P-

**Deleted:** , which we hypothesize was due to lower Fe-to-fixed nitrogen supply ratios that decrease their competitive ability with non-diazotrophic phytoplankton.

**Deleted:** nitrogen

**Deleted:** northern South China Sea (

**Deleted:** )

**Deleted:** nitrogen

**Deleted:** always

**Deleted:** diazotroph community structure

**Deleted:** , which

**Deleted:** diazotroph community

49 limited. Our study provides comprehensive evidence of nutrient controls on N<sub>2</sub> fixation  
50 biogeography in the margin of the western North Pacific. Future research that more  
51 accurately constrains nutrient supply rates to this region would be beneficial for resolving  
52 what controls diazotroph community structure.

**Formatted:** Font: 14 pt, Bold

**Deleted:** We further hypothesize the importance of absolute Fe...

**Deleted:** in regulating spatial variability in

**Deleted:** across the study area.

## 57 **1 Introduction**

58 Nitrogen fixation by diazotrophic bacteria converts abundant dinitrogen (N<sub>2</sub>) gas into  
59 ammonia, providing nearly half of the ocean's bioavailable nitrogen (N) (Gruber and  
60 Galloway, 2008), which goes on to support >30% of carbon export from surface to deep  
61 waters in the N-limited ocean (Böttjer et al., 2016; Wang et al., 2019). A diverse  
62 community of diazotrophs has been described across the oligotrophic ocean that includes  
63 *Trichodesmium*, unicellular cyanobacteria (UCYN-A and *Crocosphaera*, also referred to  
64 as UCYN-B), the heterocystous symbiont *Richelia* associated with diatoms (DDAs,  
65 diatom-diazotroph associations), and noncyanobacterial diazotrophs (NCDs,  
66 heterotrophic or photoheterotrophic bacteria) (Zehr and Capone, 2020). However, there is  
67 still a lack of knowledge on what controls diazotrophic distribution, activity and  
68 community structure in the current ocean.

69

70 Iron (Fe) and phosphorus (P) are believed to be key factors controlling the biogeographic  
71 distribution of marine N<sub>2</sub> fixation (Sohm et al., 2011; Zehr and Capone, 2020; Wen et al.,  
72 2022). Fe is particularly important for N<sub>2</sub> fixers as a cofactor for the FeS-rich  
73 nitrogenase enzyme (Berman-Frank et al., 2001), whereas P is also required for genetic  
74 information storage, cellular structure and energy generation. A number of nutrient-  
75 addition bioassay experiments conducted in the field have shown that N<sub>2</sub> fixation in the  
76 oligotrophic oceans can be limited by Fe or P, or co-limited by both nutrients at the same

77 time (Mills et al., 2004; Needoba et al., 2007; Grabowski et al., 2008; Watkins-Brandt et  
78 al., 2011; Langlois et al., 2012; [Turk-Kubo et al., 2012](#); Dekaezemacker et al., 2013;  
79 Krupke et al., 2015; Tanita et al., 2021; Wen et al., 2022). However, few studies have  
80 quantified how the supply of Fe and/or P impacts the abundance of individual  
81 diazotrophic phylotypes and their community structure (Langlois et al., 2012; Moisander  
82 et al., 2012; Turk-Kubo et al., 2012). Experiments conducted so far that investigated this  
83 were located in the South Pacific and North Atlantic, and found diverse responses among  
84 diazotrophic phylotypes to the addition of Fe and/or P. Furthermore, the responses of total  
85 diazotroph abundances assessed from *nifH* gene quantifications ~~did~~ not qualitatively  
86 match the responses of bulk N<sub>2</sub> fixation rates (Langlois et al., 2012; Moisander et al.,  
87 2012; Turk-Kubo et al., 2012). Resolution of the specific types of diazotrophs responding  
88 to nutrient supply, in addition to overall N<sub>2</sub> fixation rates, ~~is~~ potentially crucial for  
89 understanding their biogeography, which in turn could be important for biogeochemical  
90 function. For example, the presence of large *Trichodesmium* filaments is expected to have  
91 a different fate in the microbial food web and contribute differently to the sinking flux of  
92 carbon than that of small unicellular species (Bonnet et al., 2016).

Deleted: ; Turk-Kubo et al., 2012

Deleted: were

Deleted: are

93  
94 The northern South China Sea (NSCS) and the neighboring western boundary of the  
95 North Pacific are interacting water bodies, with the major western boundary Kuroshio  
96 Current intruding into the NSCS across the Luzon Strait, generating frontal zones with

100 unique physical and biogeochemical characteristics (Du et al., 2013; Guo et al., 2017; [Xu](#)  
101 [et al., 2018](#); Huang et al., 2019; Lu et al., 2019; [Li et al., 2021](#)). Common to the full  
102 regime, however, is surface waters that are warm, stratified and N-depleted, but subject to  
103 elevated dust input from the Gobi Desert (Duce et al., 1991; Jickells et al., 2005). These  
104 conditions potentially provide an ideal habitat for diazotrophs (Chen et al., 2003; Wu et  
105 al., 2003). Investigations in these regions have shown high variability in diazotroph  
106 abundances and N<sub>2</sub> fixation rates (Chen et al., 2003; Chen et al., [2008](#); Chen et al., [2014](#);  
107 [Wu et al., 2018](#); Lu et al., 2019), which overall increased from the NSCS basin to the  
108 western boundary of the North Pacific (Wen et al., 2022). Along this gradient in N<sub>2</sub>  
109 fixation, the dominant diazotroph types switched from *Trichodesmium* in the NSCS to  
110 UCYN-B in the western boundary of the North Pacific (Wen et al., 2022). Several studies  
111 have hypothesized that these gradients of diazotroph abundances and N<sub>2</sub> fixation rates  
112 were regulated by nutrient availability (specifically, Fe, P and N; Wu et al., 2003; Chen et  
113 al., 2003; Chen et al., 2008; Shiozaki et al., 2014a; Shiozaki et al., 2015a). More recent  
114 observational and experimental evidence supported the hypothesis that Fe:N supply ratios  
115 are the main drivers of the abundance of diazotrophs and N<sub>2</sub> fixation rates across the  
116 western North Pacific (Wen et al., 2022). With an increasing supply ratio of Fe:N from  
117 the North Equatorial Current (NEC) to the Philippines Sea, Wen et al. (2022) found that  
118 diazotroph abundances and N<sub>2</sub> fixation rates increased, and bioassay experiments  
119 demonstrated evidence for N<sub>2</sub> fixation rates switching from Fe to P limitation or to

Deleted: Li et al., 2021;

Deleted: Xu

Deleted: 2018

Deleted: 2014

Deleted: 2008;

Deleted: ; Wu et al., 2018

126 nutrient-replete conditions. In the NSCS, Wen et al. (2022) found N<sub>2</sub> fixation rates fell in  
127 between NEC and Kuroshio values and bioassay experiments demonstrated rates were  
128 co-limited by Fe and P, which they hypothesized was due to intermediate Fe:N supply  
129 ratios (Wen et al., 2022).

130

131 Although this previous study has outlined the broad spatial pattern of nutrient regulation  
132 of marine N<sub>2</sub> fixation throughout the western subtropical Pacific (Wen et al., 2022),  
133 important questions remain. Two specific examples are: (i) the [Kuroshio intrusion](#)  
134 [generates a frontal zone with a unique diazotrophy regime in the NSCS \(Lu et al., 2019\)](#),  
135 [and thus the](#) relatively lower spatial resolution of the experiments in Wen et al. (2022)  
136 and other studies ([Shiozaki et al., 2014b](#); [Chen et al., 2019](#)) remains insufficient to

137 delineate Fe and P controls at finer spatial scales between the neighboring NSCS and the  
138 western boundary of the North Pacific; and (ii) in addition to controls on N<sub>2</sub> fixation  
139 rates, broad-scale differences in the types of diazotrophs dominating the N<sub>2</sub> fixer  
140 community were not concretely associated with environmental drivers in experimental  
141 tests for nutrient limitation, because changes in type-specific diazotroph abundances  
142 following nutrient addition were not measured ([Shiozaki et al., 2014b](#); [Chen et al., 2019](#);

143 Wen et al., 2022). Therefore, in the present study we extend the findings of Wen et al.  
144 (2022) and others by carrying out additional, higher-spatial resolution observations of  
145 volumetric N<sub>2</sub> fixation rates and measurements of the [nifH gene](#) abundances of key

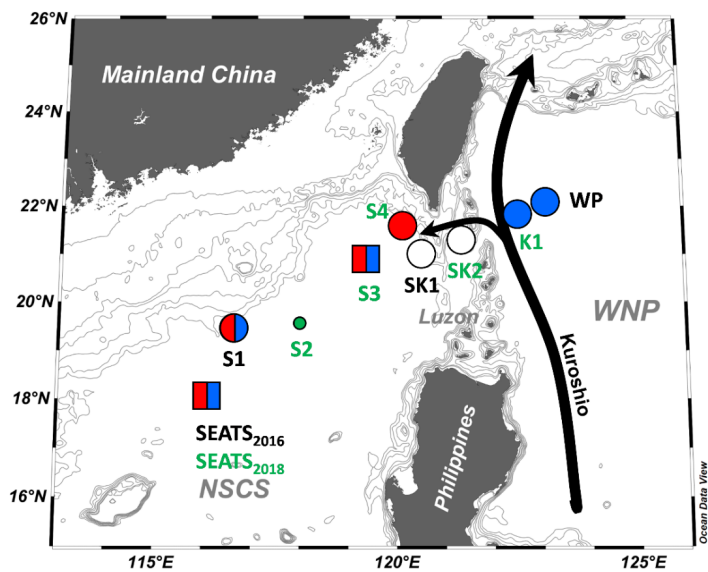
Deleted: Chen et al., 2019;

Deleted: ) remain

Deleted: Chen et al., 2019;

149 diazotrophic phylotypes from the NSCS basin to the western boundary of the North  
 150 Pacific (including the upstream Kuroshio) between 2016 and 2018 (Fig. 1). These new  
 151 observations were supplemented by a further additional eight, high volume (10 L)  
 152 nutrient amendment bioassay experiments throughout the transect to directly test the  
 153 response of both (i)  $N_2$  fixation rates, and (ii) *nifH* gene abundances to supply of  
 154 potentially limiting nutrients (Fe, P, and Fe+P).

155



156  
 157

158 **Figure 1.** Sampling and nutrient amendment experiment locations in the northern South  
 159 China Sea and the western boundary of the North Pacific. One station (SEATS<sub>2016</sub>) was  
 160 sampled in 2016, three (S1, SK1, WP) were in 2017, and six (stations with green labels)  
 161 were in 2018. Nutrient amendment experiments were conducted at 8 of 10 stations.  
 162 Symbols summarize the nutrient limitation of  $N_2$  fixation rates found at each site: red, Fe  
 163 limitation; blue, P limitation; split red/blue, Fe-P co-limitation; white, nutrient replete.



164 Co-limitation type is indicated by symbol type (square, independent co-limitation; circle,  
165 simultaneous co-limitation). WNP, the western North Pacific. Black arrows indicate  
166 Kuroshio Current and its branch.

167

## 168 **2 Method**

### 169 **2.1 Sample collection**

170 Investigations and bioassay experiments were conducted on three cruises to the NSCS  
171 (stations SETAS and S1 to S4), the Luzon Strait (stations SK1 and SK2), the upstream  
172 Kuroshio (station K1), and the western boundary of the North Pacific (station WP) (Fig.  
173 1), between May 2016 and June 2018 onboard the R/V *Dongfanghong 2* and R/V *Tan*  
174 *Kah Kee*. At each station (except station SK2 where no hydrological data are available),  
175 temperature and salinity were recorded by a Seabird 911 CTD. Water samples were  
176 collected using Niskin-X bottles at five or six depths (except SK2, only surface waters  
177 were sampled) throughout the upper 150 m for the determination of N<sub>2</sub> fixation and  
178 primary production rates. Seawaters from each depth were also sampled for the analysis  
179 of *nifH* gene abundance. Samples for nutrient analysis were also collected. Seawater for  
180 the bioassay experiments (at 8 of 10 stations) was collected using a trace-metal-clean  
181 towed sampling device located around 2-5 m depth with suction provided by a Teflon  
182 bellows pump. Seawaters were sampled in a dedicated trace-metal-clean laminar flow  
183 hood maintained over-pressurized by HEPA-filtered air. During the cruise in 2018  
184 (stations with green labels in Fig. 1), surface waters were sampled under trace-metal-

**Deleted:** Gray lines indicate 50, 100, 300, 500, 1000, 1500 and 2000 m bathymetric depth contours.

187 clean conditions for the determination of total particulate Fe concentration.

188

## 189 **2.2 N<sub>2</sub> fixation and primary production rate measurements**

190 N<sub>2</sub> fixation rates were determined by the <sup>15</sup>N<sub>2</sub> gas dissolution method (Mohr et al., 2010),

191 combined with a primary production assay using NaH<sup>13</sup>CO<sub>3</sub> (99 atom% <sup>13</sup>C, Cambridge

192 Isotope Laboratories). Briefly, 0.22 μm-filtered surface seawater was degassed using a

193 Sterapore membrane unit (20M1500A: Mitsubishi Rayon Co., Ltd., Tokyo, Japan) as

194 described in Shiozaki et al. (2015b). After that, 20 mL 98.9 atom% pure <sup>15</sup>N<sub>2</sub> gas

195 (Cambridge Isotope Laboratories) was injected into a gas-tight plastic bag ([Tedlar<sup>®</sup>PVE](#),

196 [Dalian Delin Gas Packing Co., Ltd](#)) containing 2 L of the degassed seawater and allowed

197 to fully equilibrate before use. The N<sub>2</sub> fixation and primary production incubations were

198 conducted in duplicate 4.3 L Nalgene polycarbonate bottles. Samples were spiked with

199 100 mL <sup>15</sup>N<sub>2</sub> enriched filtered seawater from the same site and incubated on-deck for 24

200 h. The final <sup>15</sup>N<sub>2</sub> enriched seawater concentration in the incubation bottles was not

201 measured directly during this study. We thus employed a <sup>15</sup>N<sub>2</sub> atom% of 1.40 ± 0.08

202 atom% ([ranges from 1.28 to 1.56 atom%](#), *n* = 17) measured in a following cruise in 2020

203 (Wen et al., 2022), during which the N<sub>2</sub> fixation incubations were conducted using the

204 same approach, reagents, and equipment as for the study described here. For primary

205 production measurements, NaH<sup>13</sup>CO<sub>3</sub> solution was added ~~to~~ a [final amended](#)

206 concentration of 100 μM. After that, the bottles were covered with a neutral-density

Deleted: at

208 screen to adjust the light to the levels at sampling depths, and then were incubated for 24  
209 h in an on-deck incubator continuously flushed with surface seawater. Incubated samples  
210 were filtered onto pre-combusted (450 °C, 4 h) GF/F filters, and the particulate organic  
211 matter from each depth were also collected to determine background POC/PON  
212 concentrations and their natural  $^{13}\text{C}/^{15}\text{N}$  abundances.

213

214 All filter samples were acid fumed to remove the inorganic carbon and then analyzed  
215 using an elemental analyzer coupled to a mass spectrometer (EA-IRMS, Thermo Fisher  
216 Flash HT 2000-Delta V plus). The  $\text{N}_2$  fixation and primary production rates were then  
217 calculated according to Montoya et al. (1996) and Hama et al. (1983), respectively. The  
218 detection limits of  $\text{N}_2$  fixation rates were then calculated according to Montoya et al.  
219 (1996), taking 4‰ as the minimum acceptable change in the  $\delta^{15}\text{N}$  of particulate nitrogen.  
220 All parameters involved in  $\text{N}_2$  fixation rate calculation are shown in Supplementary  
221 Materials. To represent the inventories, the upper 150 m depth-integrated  $\text{N}_2$  fixation rate  
222 and primary production were calculated by the trapezoidal integration method.

223

### 224 **2.3 *nifH* gene abundance**

225 At each depth, 4.3 L seawater samples for DNA extraction were filtered onto 0.22  $\mu\text{m}$   
226 pore-sized membrane filters (Supor200, Pall Gelman, NY, USA) and then frozen in liquid  
227  $\text{N}_2$ . To extract the DNA, membranes were cut into pieces under sterile conditions, and

228 then extracted using the QIAamp® DNA Mini Kit (Qiagen) following the manufacturer's  
229 protocol. The quantitative polymerase chain reaction (qPCR) analysis was targeted on the  
230 *nifH* phylotypes of *Trichodesmium* spp., unicellular cyanobacterial UCYN-A1, UCYN-  
231 A2, and UCYN-B, *Richelia* spp. (het-1), and a gamma-proteobacterium ( $\gamma$ -24774A11),  
232 using previously designed primers and probe sets (Supplementary Table S1; Church et al.,  
233 2005a; Church et al., 2005b; Moisaner et al., 2008; Thompson et al., 2014). A recent  
234 study suggested that the primers for UCYN-A2 also target UCYN-A3 and thus cannot be  
235 used to differentiate between these two phylotypes (Farnelid et al., 2016). Therefore, we  
236 used the convention UCYN-A2/A3 when referring to these two groups. The *nifH*  
237 standards were obtained by cloning the environmental sequences from previous samples  
238 collected from the SCS. qPCR analysis was carried out as described previously (Church  
239 et al., 2005a) with slight modifications. Triplicate qPCR reactions were run for each  
240 environmental DNA sample and for each standard on a CFX96 Real-Time System (Bio-  
241 Rad Laboratories). Standards corresponding to between  $10^1$  and  $10^7$  copies per well were  
242 amplified in the same 96-well plate. The amplification efficiencies of PCR were always  
243 between 90-105%, with  $R^2$  values  $> 0.99$ . The quantification limit of the qPCR reactions  
244 was 10 *nifH* gene copies per reaction, and 1  $\mu$ L from 100 or 150  $\mu$ L template DNA was  
245 applied to qPCR assay, which was equivalent to approximately ~230-350 gene copies per  
246 L of seawater sample filtered (4.3 L).

247

248 [A previous study has reported that \*nifH\* gene polyploidy exists in \*Trichodesmium\*](#)  
249 [\(Sargent et al., 2016\), which may impact the estimates of diazotroph compositions.](#)  
250 [However, given that the degree of polyploidy can vary significantly \(ranging from 1 to](#)  
251 [1405; Sargent et al., 2016; White et al., 2018\), with a potential dependence on the growth](#)  
252 [conditions, nutrient status, developmental stage, and cell cycle \(see references in](#)  
253 [Karlusich et al., 2021\), we did not attempt to account/correct for this in calculations of](#)  
254 [proportions of the different diazotrophs.](#)

#### 256 **2.4 Bioassay experiments**

257 Acid-cleaned Nalgene polycarbonate carboys (10 L) were filled with near surface  
258 seawater from the towed fish system. Trace metal clean techniques were strictly applied  
259 in experimental setup and manipulations. All materials [including the degas unit and](#)  
260 [Tedlar®PVF bags that came](#) in contact with the incubation water were acid-washed in a  
261 Class-100 cleanroom before use. Nutrient amendments at all sites were Fe, P, and Fe+P.  
262 [Surface dissolved Fe and P concentrations previously reported in the NSCS were 0.17-](#)  
263 [1.01 nM and 5-20 nM respectively \(Wu et al., 2003; Zhang et al., 2019\). In order to](#)  
264 [obtain a measurable response within the relatively short 72-hour experimental period, 2](#)  
265 [nM Fe and 100 nM P \(chelexed and filter-sterilized\) were added to each of the treatment](#)  
266 [bottles.](#) Control bottles incubated with no nutrient treatment were included in all  
267 experiments. [Treatments for 7 out of 8 experiments](#) were conducted with 3 replicates,

Deleted: coming

Deleted: The amended

Deleted: concentrations were 2 nM and 100 nM, respectively.

Deleted: All treatments

Deleted: 2 or

Deleted: and

274 [However, there were three cases when one of the triplicate samples was lost due to](#)  
275 [filtration errors \(one +Fe+P carboy at station S1, one NFR/PP sample of +Fe+P at station](#)  
276 [WP, and one NFR/PP sample of +P sample at station S3\). In addition, for the bioassay](#)  
277 [experiment at station SEATS<sub>2016</sub>, sufficient water was only available to conduct the](#)  
278 [experiment with 2 replicates for control and +Fe+P treatments, while +Fe and +P retained](#)  
279 [3 replicates. All carboys were then](#) incubated for 3 days in a screened on-deck incubator  
280 [\(a ~400-L clear on-deck incubator with inflow and outflow\)](#) continuously flushed with  
281 surface seawater. After [72 hours](#) pre-incubation, subsamples were collected for the  
282 determination of [Chl \*a\* concentration](#), N<sub>2</sub> fixation rate and *nifH* gene abundance. <sup>15</sup>N<sub>2</sub>  
283 enriched seawater was prepared as described above, except that all the materials coming  
284 in contact with the seawater were acid-cleaned before use.

285

## 286 **2.5 Macronutrient and chlorophyll *a* analyses**

287 Samples for macronutrient analyses were collected in 125-mL acid-washed high-density  
288 polyethylene (HDPE) bottles (Nalgene), and analyzed onboard using a Four-channel  
289 Continuous Flow Technicon AA3 Auto-Analyzer (Bran-Lube GmbH). The detection  
290 limits for NO<sub>3</sub><sup>-</sup>+NO<sub>2</sub><sup>-</sup> and PO<sub>4</sub><sup>3-</sup> were 0.1 μmol L<sup>-1</sup> and 0.08 μmol L<sup>-1</sup>, respectively. The  
291 nitracline was defined as the depth at which NO<sub>x</sub> concentration equaled 0.1 μmol L<sup>-1</sup> (Le  
292 Borgne et al., 2002). [Surface seawaters were additionally sampled for the measurement of](#)  
293 [low-level nutrient concentrations in the 2018 cruise and NO<sub>3</sub><sup>-</sup>+NO<sub>2</sub><sup>-</sup> was determined](#)

294 following Zhang (2000) whilst  $\text{PO}_4^{3-}$  was analyzed following Ma et al., (2008). Samples  
295 for chlorophyll *a* analysis were collected on nominal 0.7  $\mu\text{m}$  pore-size GF/F filters  
296 (Whatman), extracted in 90% acetone, and analyzed fluorometrically on a Turner Designs  
297 fluorometer (Welschmeyer 1994).

Deleted: ) and chlorophyll

Formatted: Font: Not Italic

Deleted: concentration was determined using a Trilogy

Deleted: Turner-Designs, USA).

## 299 2.6 Particulate Fe concentration

300 Total particulate Fe ( $\text{PFe}_{\text{total}}$ ) and intracellular Fe ( $\text{PFe}_{\text{intra}}$ ) were sampled under laminar  
301 flow hood. Briefly, 4-9 L of surface waters were filtered onto acid-cleaned 0.22- $\mu\text{m}$   
302 polycarbonate membrane filters. For  $\text{PFe}_{\text{intra}}$  samples, in order to remove metal bound to  
303 the cell surface, cells were exposed twice to an oxalate-EDTA solution for 5 minutes and  
304 rinsed nine times with Chelex-cleaned 0.56 mol  $\text{L}^{-1}$  NaCl solution (Li et al., 2020).  
305  $\text{PFe}_{\text{total}}$  and  $\text{PFe}_{\text{intra}}$  concentrations were then determined by ICP-MS (ICP-MS 7700X,  
306 Agilent).

Deleted: -

## 308 2.7 Statistical analysis

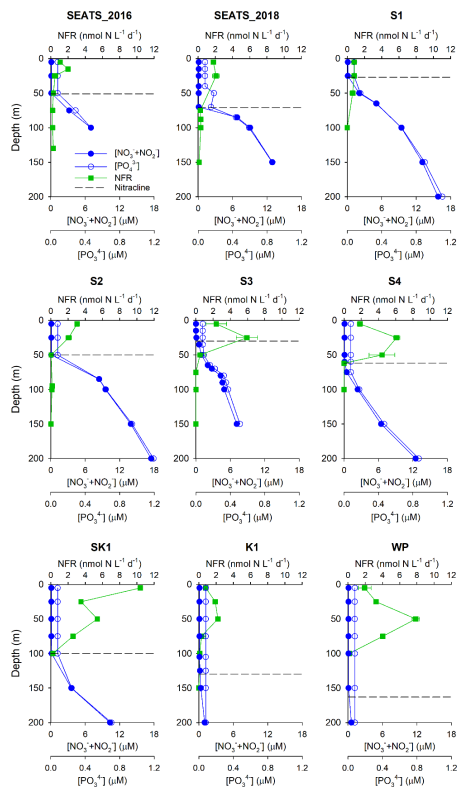
309 Significance of differences among nutrient treatments of bioassay experiments (for  $\text{N}_2$   
310 fixation rate) were tested by ANOVA followed by Fisher PSLD test, using R-4.1.2.  
311 Pairwise correlation between  $\text{N}_2$  fixation rates, diazotroph groups and environmental  
312 factors was analyzed using Pearson correlation. A significance level of  $p < 0.05$  was  
313 applied, except as noted where significance was even greater. It should be noted that

318 [those statistical results that were produced from only two replicates are not strictly](#)  
 319 [statistically valid, but for completeness the posthoc test results are nevertheless still](#)  
 320 [included here.](#)

321

### 322 3 Results

#### 323 3.1 Spatial variations of N<sub>2</sub> fixation rates and diazotroph composition



324

325

326 **Figure 2.** Vertical profiles of N<sub>2</sub> fixation rates. Green squares, N<sub>2</sub> fixation rate (NFR,

Formatted: Left



327 nmol N L<sup>-1</sup> d<sup>-1</sup>); blue solid circles, NO<sub>3</sub><sup>-</sup>+NO<sub>2</sub><sup>-</sup> concentrations (μM); blue open circles,  
 328 PO<sub>4</sub><sup>3-</sup> concentrations (μM). The dashed line indicates the nitracline depth. Note that no  
 329 profile data were available at station SK2.

330

331 [Our survey revealed substantial spatial variability in N<sub>2</sub> fixation rates and \*nifH\* gene](#)

Formatted: Left

332 abundances across the study area (Figs. 2 and 3). Vertically, high N<sub>2</sub> fixation rates were

333 found in the upper 50 m (ranged from [below](#) detection limit to 10.4 ± 0.01 nmol N L<sup>-1</sup> d<sup>-1</sup>

Deleted: below

334 <sup>1</sup>), rates dropped rapidly at greater depths (Fig. 2), and surface rates were positively

335 correlated with depth-integrated rates (Pearson  $r = 0.68$ ,  $p = 0.043$ , Supplementary Table

336 S2). Horizontally, depth-integrated N<sub>2</sub> fixation rates were generally low at the central

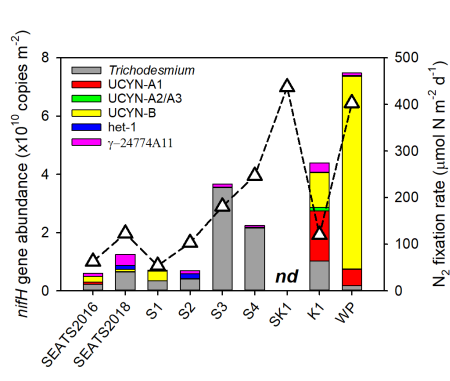
337 NSCS basin stations (SEATS, S1 and S2, on average 86 ± 33 μmol N m<sup>-2</sup> d<sup>-1</sup>), elevated at

338 stations close to the western edge of the Luzon Strait (S3 and S4, on average 214 ± 47

339 μmol N m<sup>-2</sup> d<sup>-1</sup>), and were highest at the Luzon Strait station (SK1, 437 μmol N m<sup>-2</sup> d<sup>-1</sup>)

340 and the western North Pacific boundary station (WP, 403 μmol N m<sup>-2</sup> d<sup>-1</sup>) (Figs. 1, 3 and

341 Table 1).



342

344  
 345 **Figure 3.** Depth-integrated (upper 150 m) *nifH* gene abundances (bars) and N<sub>2</sub> fixation  
 346 rates (triangles). Note that depth-integrated N<sub>2</sub> fixation rates and *nifH* gene abundances  
 347 were not available at station SK2. nd, not determined.

348  
 349 **Table 1.** Environmental conditions, N<sub>2</sub> fixation, and primary production rates. Sea  
 350 surface temperature (SST) and salinity (SSS), [chlorophyll \*a\* concentration](#), [surface](#)  
 351 [dissolved inorganic nitrogen \(SDIN\) and phosphorus \(SDIP\)](#), nitracline depth (D<sub>Nitr</sub>),  
 352 surface N<sub>2</sub> fixation rate (SNF), upper 150 m depth-integrated N<sub>2</sub> fixation rate (INF) and  
 353 primary production (IPP) at each station. nd, not determined.

Station	SST (°C)	SSS	Chl <i>a</i> (µg/L)	<a href="#">SDIN</a> (nM)	<a href="#">SDIP</a> (nM)	D <sub>Nitr</sub> (m)	SNF (nmol N L <sup>-1</sup> d <sup>-1</sup> )	INF (µmol N m <sup>-2</sup> d <sup>-1</sup> )	IPP (mmol C m <sup>-2</sup> d <sup>-1</sup> )
SEATS <sub>2016</sub>	30.3	33.46	0.26	nd	nd	51	1.1	63	44
SEATS <sub>2018</sub>	30.3	33.46	0.11	<a href="#">9.5</a>	<a href="#">16.8</a>	71	1.8	123	24
S1	29.5	33.73	0.24	nd	nd	27	0.8	54	43
S2	29.4	33.75	0.10	<a href="#">9.6</a>	<a href="#">13.0</a>	50	3.0	103	24
S3	28.7	33.53	0.15	<a href="#">11.1</a>	<a href="#">16.2</a>	30	2.4	181	98
S4	29.5	33.74	0.17	<a href="#">5.1</a>	<a href="#">11.7</a>	62	1.8	247	59
SK1	30.5	33.62	0.22	nd	nd	100	10.4	437	11
SK2	nd	nd	0.11	nd	nd	nd	2.0	nd	nd
K1	29.1	34.45	0.11	<a href="#">5.9</a>	<a href="#">16.8</a>	130	0.8	120	19
WP	30.9	34.47	0.11	nd	nd	163	1.9	403	9

Deleted:

Inserted Cells

Inserted Cells

354  
 355 A significant positive correlation was found between the depth-integrated *nifH* gene  
 356 abundance and N<sub>2</sub> fixation rate (Pearson  $r = 0.72$ ,  $p = 0.046$ , Supplementary Table S2),  
 357 demonstrating that the [nifH gene](#) abundances of these major diazotroph phylotypes [that](#)  
 358 [we surveyed](#) well explained the major variability in measured rates. However,  
 359 considerable spatial variation was found in the specific diazotrophs supporting N<sub>2</sub>

361 fixation (Fig. 3). *Trichodesmium* dominated the [total \*nifH\* gene abundance](#) throughout the  
362 water column of the NSCS (52-96% of the total *nifH* gene abundance, excluding station  
363 SEATE<sub>2016</sub>). In contrast, at the Kuroshio station K1, unicellular diazotrophic  
364 cyanobacteria (UCYN-A and UCYN-B) were the most abundant [nifH gene](#) phylotypes,  
365 and at station WP, UCYN-B alone was dominant (Fig. 3 and Supplementary Table S3). [It](#)  
366 [should be noted that \*nifH\* gene polyploidy exists in \*Trichodesmium\* \(Sargent et al., 2016\),](#)  
367 [which may have an important impact on the estimates of both in situ and nutrient-treated](#)  
368 [diazotroph compositions \(see Method\).](#)

Deleted: diazotroph assemblage

369

### 370 3.2 Diazotroph response to Fe and P supply

371 To directly test which nutrients were limiting overall N<sub>2</sub> fixation rates and the [nifH gene](#)  
372 abundances of individual diazotrophs, we conducted eight, ~3-day nutrient addition  
373 bioassay experiments (Figs. 4 and 5). The responses of N<sub>2</sub> fixation rate to different  
374 combinations of Fe and P supply demonstrated a coherent geographic switch across the  
375 study area (Figs. 1, 4 and 5). At stations towards to the NSCS basin (SEATS<sub>2016</sub>, S1 and  
376 S3), N<sub>2</sub> fixation rates were co-limited by Fe and P. Two forms of this co-limitation were  
377 identified: (i) only simultaneous Fe and P addition stimulated N<sub>2</sub> fixation rates  
378 ('simultaneous co-limitation', station S1, Fig. 4); (ii) independent addition of either Fe or  
379 P alone, or supply of Fe and P in combination, enhanced N<sub>2</sub> fixation rates ('independent  
380 co-limitation', [station SEATS<sub>2016</sub>, Fig 4](#)). [For the experiment conducted at station S3, in](#)

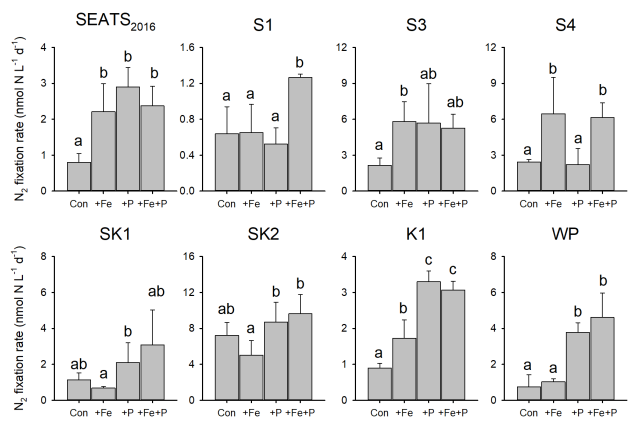
Deleted: abundance

Deleted: stations SEATS<sub>2016</sub> and S3, Fig 4).

384 [which N<sub>2</sub> fixation was also recognized to be independently co-limited, the rates in all](#)  
 385 [nutrient-amended groups increased by 1.44-1.70 times compared to control values,](#)  
 386 [although statistical significances were not observed in +P and +Fe+P treatments \(Fig. 4\).](#)  
 387 Further to the northeast, in contrast, N<sub>2</sub> fixation rates were only stimulated by nutrient  
 388 combinations containing Fe at S4 and by combinations containing P at K1 and WP,  
 389 suggesting single limitation by Fe or P, respectively, at these sites (Fig. 4). Although Fe  
 390 addition also appeared to stimulate N<sub>2</sub> fixation rates at station K1, P was generally the  
 391 major limiting nutrient at this station taking into account the responses of both N<sub>2</sub> fixation  
 392 rates and *nifH* gene abundance (see below) (Figs. 4 and 5). At stations SK1 and SK2 in  
 393 the Luzon Strait, mean N<sub>2</sub> fixation rates [and \*nifH\* gene abundances](#) were not significantly  
 394 [affected by nutrient amendments](#), suggesting that both Fe and P availability were not  
 395 limiting N<sub>2</sub> fixation rates (Figs. 4 and 5).

Deleted: (  
 Deleted: )  
 Deleted: were highest in treatments containing P, but responses...  
 Deleted: greater than the untreated controls  
 Deleted: Fig

396



397

404

405 **Figure 4.** Response of N<sub>2</sub> fixation to nutrient amendment. Error bars represent the  
406 standard deviation of biological replicates ( $n = 2$  or  $3$ ). Different letters above error bars  
407 indicate statistically significant differences ( $p < 0.05$ ) between treatments (ANOVA  
408 followed by Fisher PLSD test). Note that statistical results were produced from only two  
409 replicates for control and +Fe+P at station SEATS<sub>2016</sub>, +Fe+P at stations S1 and WP, and  
410 +P at station S3, and should thus be treated with caution.

411

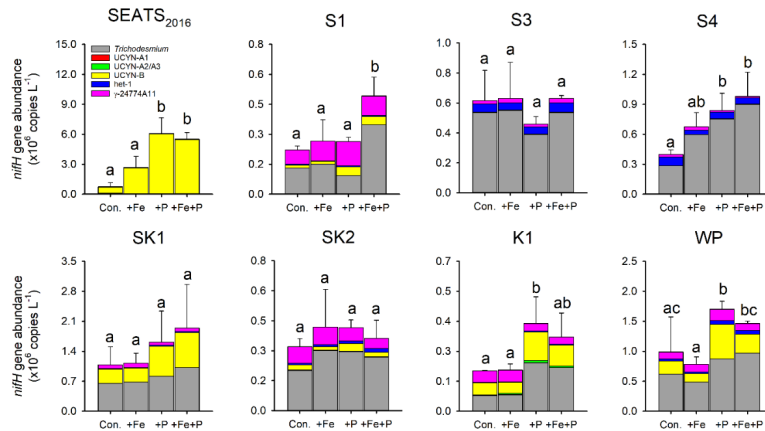
412 Further detail as to the drivers of the N<sub>2</sub> fixation responses to Fe and P additions was  
413 provided by the species-level analysis of diazotroph *nifH* from the treatment bottles. In  
414 general, responses of total *nifH* gene abundance to Fe and P amendments were  
415 qualitatively consistent with N<sub>2</sub> fixation rates at most sites, that is, the nutrient(s) limiting  
416 N<sub>2</sub> fixation rates also limited the diazotroph *nifH* abundance (Figs. 4 and 5). The  
417 exceptions were at stations S3 and S4, where variability in *nifH* abundances was observed  
418 in response to nutrient treatment (station S3) or overall trends differed between *nifH*  
419 abundances and N<sub>2</sub> fixation rates (station S4; enhanced *nifH* abundance in response to +P,  
420 whereas rates only responded to +Fe). Quantitatively, the responses of N<sub>2</sub> fixation rates  
421 and *nifH* biomass to nutrient addition were not well correlated (total *nifH* abundance  
422 increase rate, calculated as  $\text{Ln}(nifH_{\text{treatment}}/nifH_{\text{control}})/\text{incubation time}$ , versus the  
423 N<sub>2</sub> fixation increase rate following nutrient supply,  $R^2 = 0.07$ ,  $p = 0.21$ ; Supplementary  
424 Fig. S1), despite initial background *nifH* abundances and N<sub>2</sub> fixation rates being well  
425 correlated (Pearson  $r = 0.72$ ,  $p = 0.046$ , Supplementary Table S1). This suggested a  
426 decoupling of the rates of change in biomass and N<sub>2</sub> fixation rates following nutrient

Formatted: Left

Deleted: versus

428 addition over the relative short incubation timescales (~3 days).

429



430

431

432 **Figure 5.** Response of diazotroph phylotypes to nutrient amendment. Bar heights  
433 represent the mean total *nifH* concentration and error bars the standard deviation of  
434 biological replicates ( $n = 2$  or  $3$ ). Different letters above error bars indicate a statistically  
435 significant difference ( $p < 0.05$ ) between treatments (ANOVA followed by Fisher PLSD  
436 test). Note that statistical results were produced from only two replicates for control and  
437 +Fe+P at station SEATS<sub>2016</sub>, control and +Fe+P at station S1, and +P and +Fe+P at station  
438 SK2, and should thus be treated with caution.

439

440 Overall, the composition of the six diazotroph phylotypes that we surveyed were not

441 greatly changed after nutrient amendments (Fig. 5). *Trichodesmium* and UCYN-B were

442 the two most dominant *nifH* phylotypes in all experimental waters that contributed to the

443 enhanced total *nifH* gene abundance after nutrient additions (Figs. 3, 5 and

444 Supplementary Fig. S1). Despite showing independent co-limitation in response to Fe and

445 P supply at station SEATS<sub>2016</sub> (Fig. 4), as reflected by equally responding  $N_2$  fixation

Deleted: community structure was

Deleted: species

448 rates, UCYN-B, the dominant [nifH phylotype](#) in non-amended control waters, increased  
449 2-fold more following P addition in comparison to Fe addition (Fig. 5 and Supplementary  
450 Fig. S2). Furthermore, no significant changes in *nifH* were observed at station S3, where  
451 N<sub>2</sub> fixation rates were also independently Fe-P co-limited. More consistent between the  
452 N<sub>2</sub> fixation rates and *nifH* biomass changes were the *nifH* responses at station S1, with  
453 overall *nifH* concentrations only responding to Fe+P additions, matching the N<sub>2</sub> fixation  
454 response. This was mostly driven by co-limitation of *Trichodesmium*, whereas UCYN-B  
455 responded only to P supply (Fig. 5 and Supplementary Fig. S2).

456

457 In contrast to the Fe limitation of N<sub>2</sub> fixation rates found at station S4, *nifH* abundances  
458 showed the most significant responses to the combined supply of Fe and P. However, at  
459 sites where N<sub>2</sub> fixation rates were P-limited (K1 and WP) overall *nifH* concentrations also  
460 responded most to P addition, with contributions from both *Trichodesmium* and UCYN-B  
461 (Fig. 5). In addition, *het-1* also increased significantly with +P combinations at stations  
462 K1 and WP (Supplementary Fig. S2). By contrast,  $\gamma$ -24774A11, which also accounted for  
463 a substantial fraction of the [total \*nifH\* gene abundance](#) (up to 31%), did not show clear  
464 enhancement to nutrient additions (Supplementary Fig. S2), suggesting that it was not Fe-  
465 and/or P-limited. [Interestingly, UCYN-A disappeared in the nutrient amendment](#)  
466 [experiments, although they were abundant in the initial water at stations K1 and WP](#)  
467 [\(Figs. 3 and 5\), possibly due to an unconstrained bottle effect \(Göran et al., 2003\).](#)

Deleted: diazotroph

Deleted: diazotroph community

470

#### 471 **4 Discussion**

472 In the present study, surface dissolved inorganic nitrogen (DIN) and phosphorus (DIP)  
473 concentrations in our study area were depleted (5.1-11.1 nM DIN, 11.7-16.8 nM DIP,  
474 Table 1). Furthermore, bioassay incubations shown no significant responses of Chl *a*  
475 concentration to the amendments of Fe and/or P (Supplementary Fig. S3), together  
476 implying the overall phytoplankton community across entire area was N-limited and the  
477 upper waters were favorable for N<sub>2</sub> fixation. However, the rates and *nifH* gene  
478 abundances were much higher in the northeast region of our study area than in the NSCS  
479 basin (Fig. 3). Rates at stations SK1 and WP were comparable to those recently reported  
480 in this region (~450 μmol N m<sup>-2</sup> d<sup>-1</sup>) measured using the same <sup>15</sup>N<sub>2</sub> gas dissolution  
481 method (Lu et al., 2019; Wen et al., 2022). Although relatively low rates were measured  
482 at the Kuroshio Current station (K1) compared with previous observations (e.g., Wen et  
483 al., 2022), high *nifH* gene abundance was nevertheless observed at this site (Fig. 3 and  
484 Supplementary Table S3). Therefore, our observations provide increasing evidence for  
485 this western (sub)tropical North Pacific boundary region containing important “hot spots”  
486 of N<sub>2</sub> fixation (Shiozaki et al., 2010; Shiozaki et al., 2015a; Wen et al., 2022). However,  
487 the elevated total *nifH* concentration in the western boundary of the North Pacific during  
488 our study was largely attributed to an increased *nifH* abundance of unicellular diazotrophs  
489 (UCYN-A and B, Fig. 3), but not *Trichodesmium* as previously reported (Chen et al.,

Deleted: In the present study,



491 2003; Chen et al., [2008](#); Chen et al., [2014](#); Shiozaki et al., 2014a). Instead, we found that  
492 *Trichodesmium nifH gene* was most abundant at stations (S3 and S4) close to the western  
493 edge of the Luzon Strait (Fig. 3 and Supplementary Table S3), where Kuroshio intrusion  
494 water has been hypothesized to introduce *Trichodesmium* into a favorable biogeographic  
495 regime (Lu et al., 2019). Either this region is spatially and/or temporally heterogeneous  
496 with respect to the presence of unicellular versus *Trichodesmium* diazotrophs, or the  
497 environmental changes have led to a shift in diazotroph community structure (Gruber,  
498 2011; Hutchins and Fu, 2017).

499

500 Depth-integrated N<sub>2</sub> fixation rate and *nifH* gene abundance were not correlated with sea  
501 surface temperature (SST), but a significant positive correlation was found between  
502 nitracline depth and total *nifH* gene abundance (Pearson  $r = 0.74$ ,  $p = 0.037$ ,  
503 Supplementary Table S2). This was suggestive of subsurface N supply into the euphotic  
504 zone, which is inversely related to nitracline depth, potentially being important in  
505 regulating diazotroph abundance in our study area, with lower N supply leading to  
506 enhanced diazotroph abundances (Chen et al., 2003; Shiozaki et al., 2014b). The presence  
507 of diazotrophs in the ocean will be a function of how well they can compete with non-  
508 diazotrophic phytoplankton for limiting resources (e.g., Fe and P) under grazing pressure  
509 ([Ward et al., 2013](#); Dutkiewicz et al., 2014; Landolfi et al., 2021). Accordingly, because  
510 of the growth characteristics of diazotrophs in comparison to non-diazotrophs, in

Deleted: 2014

Deleted: 2008

Deleted: ; Ward et al., 2013

514 particular their lack of requirement for pre-fixed N, but higher requirement for Fe and P,  
515 the relative supply rates of N, Fe and P are highly important in dictating where  
516 diazotrophs can succeed (Ward et al., 2013). Aligning with earlier global model  
517 predictions (Ward et al., 2013), and investigations in the (sub)tropical Atlantic (Schlosser  
518 et al., 2014), Wen et al. (2022) recently found that the Fe:N supply ratio (including  
519 subsurface and aerosol N and Fe supplies) was a robust predictor of diazotroph standing  
520 stock across the broader western North Pacific, including our study region.

521

522 By carrying out bioassay incubations, we observed that N<sub>2</sub> fixation rates in the NSCS  
523 basin were either (i) ‘simultaneously co-limited’ by Fe and P (identified at station S1),  
524 which represents a state where two, non-substitutable nutrients (in this case, Fe and P)  
525 have been drawn down to equally limiting levels (Sperfeld et al., 2016), or (ii)  
526 ‘independently co-limited’ (stations SEATS<sub>2016</sub> and S3), which represents a state where  
527 the resources are substitutable at biochemical (Saito et al., 2008), or community levels  
528 (Arrigo, 2005). Previous studies reported relatively low surface Fe concentrations in the  
529 NSCS basin (0.2-0.3 nM; Wu et al., 2003; Wen et al., 2022), although Fe supply rates to  
530 this region are likely elevated via riverine, sedimental and aerosol inputs (Duce et al.,  
531 1991; Jickells et al., 2005; Zhang et al., 2019). Wu et al (2003) hypothesized that the low  
532 Fe concentrations were due to a lack of Fe-binding organic ligands, which was  
533 subsequently restricting the growth of diazotrophs. We suggest that this may also be

**Deleted:** Although the current study lacked the data to calculate nutrient supply rates into the euphotic zone (matching Fe concentration profiles, euphotic depths), the correlation found between *nifH* and nitracline depth suggested the potential for the same driver (i.e., Fe:N supply rates) to be operating over this smaller spatial scale. In line with Wen et al. (2022), we further hypothesize that the expected significant N supply rate to surface waters of the NSCS (due to a shallower nitracline, alongside riverine and aerosol inputs) reduces, but does not eliminate the competitive ability of diazotrophs, as Fe supply rates to this region are likely also high

**Moved down [1]:** (Duce et al., 1991; Jickells et al., 2005;

**Moved down [2]:** 2005; Zhang et al.,

**Deleted:** 2019), thereby maintaining Fe:N supply ratios at levels supporting diazotrophs (Ward et al., 2013; Wen et al., 2022). At these Fe:N supply levels, we observed that N<sub>2</sub> fixation rates

**Moved (insertion) [1]**

**Moved (insertion) [2]**

**Deleted:** biogeochemical

553 [attributed to the rapid consumption of Fe \(as well as P\) by the faster-growing non-](#)  
554 [diazotrophs under elevated N supply \(due to shallower nitraclines, alongside riverine and](#)  
555 [aerosol inputs\). Thus we hypothesize that with the lower Fe:N supply ratio, diazotrophs](#)  
556 [in this region were outcompeted by non-diazotrophic phytoplankton and co-limited by](#)  
557 [both Fe and P \(Fig. 4\). These results add to increasing evidence for the potentially](#)  
558 [widespread Fe-P colimitation of N<sub>2</sub> fixation under elevated Fe supply \(Mills et al., 2004;](#)  
559 [Snow et al., 2015; Cerdan-Garcia et al., 2022\).](#)

560

561 The measured contributions of individual diazotrophs to total *nifH* concentration in  
562 response to nutrient supply suggested that simultaneous Fe-P co-limitation of N<sub>2</sub> fixation  
563 rates at station S1 was via regulation of *Trichodesmium*, which only responded to Fe+P  
564 addition (Fig. 5). The *nifH* responses also suggested that independent Fe-P co-limitation  
565 of N<sub>2</sub> fixation rates at sites SEATS<sub>2016</sub> and S3 was not operating at the community level  
566 (i.e., one diazotroph type limited by Fe and the other by P; [Arrigo, 2005](#)), as different  
567 [qPCR-based](#) diazotroph community structure responses to either Fe or P addition were  
568 not observed (Fig. 5). We suggest three possible causes for this observation: (i) co-  
569 limitation was at the biochemical rather than community level (i.e., either Fe or P could  
570 enhance the rates of processes ultimately driving elevated N<sub>2</sub> fixation; [Saito et al., 2008](#)).  
571 [For instance, in addition to serving as a cofactor in nitrogenase, Fe is also a cofactor in](#)  
572 [alkaline phosphatases \(Rodriguez et al., 2014; Yong et al., 2014\). Thus, the addition of Fe](#)

Deleted: ) (

Deleted: ) (Saito et al., 2008); (ii) a more subtle community co-limitation was occurring at the level of ecotypes not resolved by the *nifH* qPCR analyses

577 [may allow for enhanced utilization of dissolved organic P \(DOP\) under depleted DIP](#)  
578 [\(Browning et al., 2017\); \(ii\) other diazotrophs, which were not analyzed by the qPCR](#)  
579 [assay, may be responsible for the enhanced N<sub>2</sub> fixation rates after nutrient additions](#); or  
580 (iii) community co-limitation of N<sub>2</sub> fixation rates for the measured groups was occurring,  
581 but, unlike the simultaneous co-limitation scenario at station S1, experimental durations  
582 were too short for this to be reflected in diazotroph biomass changes. Surprisingly,  
583 stations with independent co-limitation of N<sub>2</sub> fixation rates by Fe and P (SEATS<sub>2016</sub> and  
584 S3) were not additive (i.e., increases in N<sub>2</sub> fixation rates in Fe+P treatments were not  
585 larger than Fe and P alone; Sperfeld et al., 2016). Although the available data do not  
586 allow us to provide a concrete reason for this, [the absence of this additive response may](#)  
587 [reflect one or a combination of \(i\) addition of Fe or P leading to the depletion of another](#)  
588 [secondary limitation nutrient \(e.g., Ni\), \(ii\) overall light levels setting an upper limit of N<sub>2</sub>](#)  
589 [fixation rates, which prevented further enhancements after nutrient additions, or \(iii\)](#)  
590 [grazer regulation of diazotroph biomass accumulation.](#)

591  
592 In contrast to the more central NSCS, [the deeper nitraclines](#) in the western boundary of  
593 the North Pacific, [appeared more favorable for N<sub>2</sub> fixation](#) (Fig. 3 and Table 1). [P](#)  
594 [limitation of N<sub>2</sub> fixation at these sites implied that Fe supply \(e.g., via aerosols\)](#)  
595 [stimulated diazotroph growth](#) (Fig. 3; Wen et al., 2022) [and subsequently drawdown P to](#)  
596 [limiting levels](#) (Table 1, Figs 4 and 5; Hashihama et al., 2009; Ward et al., 2013; Wen et

Deleted: ) (

Deleted: it could reflect serial limitation of N<sub>2</sub> fixation by another resource (e.g., a different nutrient or light).

Deleted: , elevated Fe:N supply ratios are expected as a result of deepening nitraclines

Deleted: 2

Deleted: ) and continued aerosol Fe inputs (

Moved (insertion) [3]

604 [al., 2022](#)). Additional Fe inputs other than aerosol deposition [are](#) also [potentially](#)  
605 [important in supporting the elevated N<sub>2</sub> fixation](#) in the Luzon Strait. At station SK2, much  
606 higher surface particulate Fe concentrations (both intracellular and total forms) were  
607 observed (Supplementary Table S4), implying [supplementary](#) Fe inputs, [potentially](#)  
608 sourced from the adjacent islands and the surrounding shallow sub-surface bathymetry  
609 (Shiozaki et al., 2014a; Shiozaki et al., 2015a).  
610  
611 In addition to the Fe:N supply ratio regulating the total *nifH* gene abundance and activity  
612 (Wen et al., 2022), we also further hypothesize that overall Fe supply rates might be an  
613 important factor in determining the diazotroph community structure in our study area  
614 (Church et al., 2008; Langlois et al., 2008; Shiozaki et al., 2017). Specifically, the depth-  
615 integrated diazotroph compositions [of the six phylotypes](#) switched from being co-  
616 dominated by *Trichodesmium* and other diazotrophs in the central NSCS (SEATS, S1 and  
617 S2), *Trichodesmium*-dominated in the more northern NSCS (S3 and S4), and finally  
618 dominated by UCYN-B in the western boundary of the North Pacific (Fig. 3 and  
619 Supplementary Table S3). Elevated Fe supply in the NSCS, particularly around the  
620 islands and shallow bathymetry of the Luzon Strait, might create a more favorable  
621 condition for *Trichodesmium* (Fig. 3 and Supplementary Table S3), consistent with  
622 elevated Fe demands of this species ([Kustka et al., 2003](#); Kupper et al., 2008; Sohm et al.,  
623 2011), as well as its ability to use particulate Fe forms (Rubin et al., 2011), and in line

Deleted: ).

Deleted: may have

Deleted: contributed to further enhanced Fe:N supply

Deleted: additional

Deleted: ,

Deleted: In turn we hypothesize that elevated Fe:N supply rates enhance N<sub>2</sub> fixation rates at these sites (Fig. 3), which leads to P drawdown and subsequent P limitation of the enhanced diazotroph stock (Figs. 4 and 5;

Moved up [3]: Hashihama et al., 2009; Ward et al., 2013; Wen et al., 2022).

635 with the elevated contribution of this species found in other regions with enhanced Fe  
636 supply (e.g., the tropical North Atlantic and western South Pacific; Sañudo-Wilhelmy et  
637 al., 2001; Sohm et al., 2011; [Bonnet et al. 2018](#); Stenegren et al., 2018). [In fact, Fe](#)  
638 [stimulation of \*Trichodesmium nifH\* abundance was observed in the experiment conducted](#)  
639 [at station S4 \(Supplementary Fig. S2\). At station S3, however, this was only observed for](#)  
640 [N<sub>2</sub> fixation rates but not \*Trichodesmium nifH\* abundance \(Supplementary Fig. S2\). We](#)  
641 [suggest this could reflect a variable decoupling of N<sub>2</sub> fixation rates and diazotroph](#)  
642 [abundance, depending on other environmental and/or ecological conditions.](#) Conversely,  
643 unicellular species may be more competitive than *Trichodesmium* in regions with lower  
644 Fe supply rates (Fig. 3). In addition to having a higher surface to volume ratio that favors  
645 Fe uptake (Hudson and Morel 1990; Jacq et al., 2014), UCYN-B species such as  
646 *Crocospaera* have been reported to employ a repertoire of Fe-conservation strategies,  
647 e.g., daily synthesis and breakdown of metalloproteins to recycle Fe between the  
648 photosynthetic and N<sub>2</sub> fixation metalloenzymes and increased expression of flavodoxin at  
649 night even under Fe-replete conditions (Saito et al., 2011). These potentially explain why  
650 UCYN-B was less Fe-limited in the NSCS basin (stations SEATS<sub>2016</sub> and S1; Fig. 5 and  
651 Supplementary Fig. S2) and dominates the diazotroph community on the western Pacific  
652 side of the Luzon Strait (Fig. 3; Chen et al., 2019; Wen et al., 2022). [Future work with](#)  
653 [paired measurements of Fe supply rates to surface waters and diazotroph community](#)  
654 [structure throughout the region would allow for more robust testing of this hypothesis.](#)

655

## 656 **5 Conclusions**

657 Observations and experiments conducted in the NSCS and the western boundary of the  
658 North Pacific demonstrated that in the more central NSCS, Fe and P were co-limiting the  
659 lower overall observed N<sub>2</sub> fixation rates, whereas P was limiting the higher rates on the  
660 western Pacific side of the Luzon Strait. This matched the expectation of higher Fe:N  
661 supply ratios in the western Pacific generating a more favorable niche for diazotrophs,  
662 leading to a drawdown of *P. Trichodesmium* and UCYN-B were the most dominant *nifH*  
663 [phylotypes](#) in the incubation waters and both dominated the responses of the total *nifH*  
664 gene after nutrient amendments. In general, nutrient addition had a relatively restricted  
665 impact on [qPCR-based](#) diazotroph community structure apart from on UCYN-B, which  
666 showed increased contribution in the diazotroph community following P addition at sites  
667 where N<sub>2</sub> fixation rates were P-limited. We hypothesize that overall switches in  
668 diazotroph community structure from *Trichodesmium*-dominated in the NSCS to single-  
669 celled UCYNA/B was related to declines in overall Fe supply rates and the different  
670 physiological strategies of these diazotrophs to obtain and use Fe. Future research that  
671 more accurately constrains nutrient supply rates to these different regions would be  
672 beneficial for further resolving this hypothesis.

Deleted: diazotroph types

674 *Data availability.* All data needed to evaluate the conclusions in the paper are present in  
675 the paper and/or the Supplementary Materials. Additional data associated with the paper  
676 are available from the corresponding authors upon request.

677

678 *Author contributions.* D.S., H.H., and Z.W. designed the research. Z.W., R.D., W.W.,  
679 W.L., X.H., W.L., and L.W. performed the experiments. Z.W., D.S., H.H., T.J.B., X.L.,  
680 and Z.C. analyzed the data. Z.W., T.J.B., H.H., and D.S. wrote the manuscript. All authors  
681 discussed the results and commented and edited the manuscript.

682

683 *Competing interests.* The authors declare that they have no conflict of interest.

684

685 *Acknowledgements.* The authors acknowledge the captains and crew of the R/V  
686 *Dongfanghong 2* and R/V *Tan Kah Kee* for the help during the cruises. This work was  
687 supported by the National Science Foundation of China (41890802, 42076149,  
688 41925026, 42106041, and 41721005), the “111” Project (BP0719030), and the  
689 XPLORER Prize from the Tencent Foundation to D. Shi.



690 **References**

- 691 Arrigo, K. R.: Marine microorganisms and global nutrient cycles, *Nature*, 437, 349-355,  
692 10.1038/nature04158, 2005.
- 693 Berman-Frank, I., Cullen, J. T., Shaked, Y., Sherrell, R. M., and Falkowski, P.: Iron  
694 availability, cellular iron quotas, and nitrogen fixation in *Trichodesmium*, *Limnol.*  
695 *Oceanogr.*, 46, 1249-1260, 10.4319/lo.2001.46.6.1249, 2001.
- 696 Bonnet, S., Baklouti, M., Gimenez, A., Berthelot, H., and Berman-Frank, I.:  
697 Biogeochemical and biological impacts of diazotroph blooms in a low-nutrient,  
698 low-chlorophyll ecosystem: synthesis from the VAHINE mesocosm experiment  
699 (New Caledonia), *Biogeosciences*, 13, 4461-4479, 10.5194/bg-13-4461-2016, 2016.
- 700 Bonnet, S., Caffin, M., Berthelot, H., Grosso, O., Benavides, M., Helias-Nunige, S.,  
701 Guieu, C., Stenegren, M., and Foster, R. A.: In-depth characterization of diazotroph  
702 activity across the Western Tropical South Pacific hot spot of N<sub>2</sub> fixation  
703 (OUTPACE cruise), *Biogeosciences*, 15, 4215-4232, 10.5194/bg-15-4215-2018,  
704 2018.
- 705 [Boström, K. H., Simu, K., Hagström, Å., and Riemann, L.: Optimization of DNA](#)  
706 [extraction for quantitative marine bacterioplankton community analysis, \*Limnol.\*](#)  
707 [\*Oceanogr.-Methods\*, 2, 365-373, 10.4319/lom.2004.2.365, 2004.](#)
- 708 Böttjer, D., Dore, J. E., Karl, D. M., Letelier, R. M., Mahaffey, C., Wilson, S. T., Zehr, J.  
709 P., and Church, M. J.: Temporal variability of nitrogen fixation and particulate

710 nitrogen export at Station ALOHA, *Limnol. Oceanogr.*, 62, 200-216,  
711 10.1002/lno.10386, 2016.

712 [Browning, T. J., Achterberg, E. P., Yong, J. C., Rapp, I., Utermann, C., Engel, A., and](#)  
713 [Moore, C. M.: Iron limitation of microbial phosphorus acquisition in the tropical](#)  
714 [North Atlantic, \*Limnol. Oceanogr. Lett.\*, 8, 15465, 10.1038/ncomms15465, 2017.](#)

715 [Cerdan-Garcia, E., Baylay, A., Polyviou, D., Woodward, E. M. S., Wrightson, L.,](#)  
716 [Mahaffey, C., Lohan, M. C., Moore, C. M., Bibby, T. S., and Robidart, J. C.:](#)  
717 [Transcriptional responses of \*Trichodesmium\* to natural inverse gradients of Fe and P](#)  
718 [availability, \*Isme J.\*, 16, 1055-1064, 10.1038/s41396-021-01151-1, 2022.](#)

719 Chen, M., Lu, Y., Jiao, N., Tian, J., Kao, S. J., and Zhang, Y.: Biogeographic drivers of  
720 diazotrophs in the western Pacific Ocean, *Limnol. Oceanogr.*, 64, 1403-1421,  
721 10.1002/lno.11123, 2019.

722 Chen, Y. L. L., Chen, H. Y., and Lin, Y. H.: Distribution and downward flux of  
723 *Trichodesmium* in the South China Sea as influenced by the transport from the  
724 Kuroshio Current, *Mar. Ecol. Prog. Ser.*, 259, 47-57, 10.3354/meps259047, 2003.

725 Chen, Y. L. L., Chen, H. Y., Tuo, S. H., and Ohki, K.: Seasonal dynamics of new  
726 production from *Trichodesmium* N<sub>2</sub> fixation and nitrate uptake in the upstream  
727 Kuroshio and South China Sea basin, *Limnol. Oceanogr.*, 53, 1705-1721,  
728 10.4319/lo.2008.53.5.1705, 2008.

729 Chen, Y. L. L., Chen, H. Y., Lin, Y. H., Yong, T. C., Taniuchi, Y., and Tuo, S. H.: The

730 relative contributions of unicellular and filamentous diazotrophs to N<sub>2</sub> fixation in  
731 the South China Sea and the upstream Kuroshio, Deep Sea Research Part I, 85, 56-  
732 71, 10.1016/j.dsr.2013.11.006, 2014.

733 Church, M. J., Björkman, K., and Karl, D.: Regional distributions of nitrogen-fixing  
734 bacteria in the Pacific Ocean, Limnol. Oceanogr., 53, 63-77, 2008.

735 Church, M. J., Jenkins, B. D., Karl, D. M., and Zehr, J. P.: Vertical distributions of  
736 nitrogen fixing phylotypes at Stn ALOHA in the oligotrophic North Pacific Ocean,  
737 Aquat. Microb. Ecol., 38, 3-14, 10.3354/ame038003 2005a.

738 Church, M. J., Short, C. M., Jenkins, B. D., Karl, D. M., and Zehr, J. P.: Temporal  
739 patterns of nitrogenase gene (*nifH*) expression in the oligotrophic North Pacific  
740 Ocean, Appl. Environ. Microbiol., 71, 5362-5370, 10.1128/AEM.71.9.5362-  
741 5370.2005, 2005b.

742 Dekaezemacker, J., Bonnet, S., Grosso, O., Moutin, T., Bressac, M., and Capone, D. G.:  
743 Evidence of active dinitrogen fixation in surface waters of the eastern tropical  
744 South Pacific during El Niño and La Niña events and evaluation of its potential  
745 nutrient controls, Global Biogeochem. Cycles, 27, 768-779, 10.1002/gbc.20063,  
746 2013.

747 Du, C., Liu, Z., Dai, M., Kao, S. J., Cao, Z., Zhang, Y., Huang, T., Wang, L., and Li, Y.:  
748 Impact of the Kuroshio intrusion on the nutrient inventory in the upper northern  
749 South China Sea: Insights from an isopycnal mixing model, Biogeosciences, 10,

750 6419-6432, 10.5194/bg-10-6419-2013, 2013.

751 Duce, R. A., Liss, P. S., Merrill, J. T., Atlas, E. L., Buat-Menard, P., Hicks, B. B., Miller,  
752 J. M., Prospero, J. M., Arimoto, R., Church, T. M., Ellis, W., Galloway, J. N.,  
753 Hansen, L., Jickells, T. D., Knap, A. H., Reinhardt, K. H., Schneider, B., Soudine,  
754 A., Tokos, J. J., Tsunogai, S., Wollast, R., and Zhou, M.: The atmospheric input of  
755 trace species to the world ocean, *Global Biogeochem. Cycles*, 5, 193-259,  
756 10.1029/91gb01778, 1991.

757 Dutkiewicz, S., Ward, B. A., Scott, J., and Follows, M. J.: Understanding predicted shifts  
758 in diazotroph biogeography using resource competition theory, *Biogeosciences*, 11,  
759 5445-5461, 10.5194/bg-11-5445-2014, 2014.

760 Farnelid, H., Turk-Kubo, K., Muñoz-Marín, M. C., and Zehr, J. P.: New insights into the  
761 ecology of the globally significant uncultured nitrogen-fixing symbiont UCYN-A,  
762 *Aquat. Microb. Ecol.*, 77, 125-138, 10.3354/ame01794, 2016.

763 [Göran, E. and Cooper, S. D.: Scale effects and extrapolation in ecological experiments,](#)  
764 [Adv. Ecol. Res., 33, 161-213, 10.1016/S0065-2504\(03\)33011-9, 2003.](#)

765 Grabowski, M. N. W., Church, M. J., and Karl, D. M.: Nitrogen fixation rates and  
766 controls at Stn ALOHA, *Aquat. Microb. Ecol.*, 52, 175-183, 10.3354/ame01209,  
767 2008.

768 Gruber, N.: Warming up, turning sour, losing breath: ocean biogeochemistry under global  
769 change, *Philos T R Soc A*, 369, 1980-1996, 10.1098/rsta.2011.0003, 2011.

770 Gruber, N. and Galloway, J. N.: An Earth-system perspective of the global nitrogen cycle,  
771 Nature, 451, 293-296, 10.1038/nature06592, 2008.

772 Guo, L., Xiu, P., Chai, F., Xue, H. J., Wang, D. X., and Sun, J.: Enhanced chlorophyll  
773 concentrations induced by Kuroshio intrusion fronts in the northern South China  
774 Sea, Geophys. Res. Lett., 44, 11565-11572, 10.1002/2017GL075336, 2017.

775 Hama, T., Miyazaki, T., Ogawa, Y., Iwakuma, T., Takahashi, M., Otsuki, A., and  
776 Ichimura, S.: Measurement of photosynthetic production of a marine phytoplankton  
777 population using a stable <sup>13</sup>C isotope., Mar. Biol., 73, 31-36, 10.1007/BF00396282,  
778 1983.

779 Hashihama, F., Furuya, K., Kitajima, S., Takeda, S., Takemura, T., and Kanda, J.: Macro-  
780 scale exhaustion of surface phosphate by dinitrogen fixation in the western North  
781 Pacific, Geophys. Res. Lett., 36, L03610, 10.1029/2008gl036866, 2009.

782 Huang, Y., Laws, E. A., Chen, B., and Huang, B.: Stimulation of heterotrophic and  
783 autotrophic metabolism in the mixing zone of the Kuroshio Current and northern  
784 South China Sea: Implications for export production, [J Geophys Res-](#)  
785 [Biogeosciences](#), 124, 2645-2661, 10.1029/2018jg004833, 2019.

786 Hudson, R. J. M. and Morel, F. M. M.: Iron transport in marine-phytoplankton - kinetics  
787 of cellular and medium coordination reactions, Limnol. Oceanogr., 35, 1002-1020,  
788 10.4319/lo.1990.35.5.1002, 1990.

789 Hutchins, D. A. and Fu, F.: Microorganisms and ocean global change, [Nat. Microbiol.](#), 2,

Deleted: Journal of Geophysical Research:

Deleted: Nature microbiology,

792 17058, 10.1038/nmicrobiol.2017.58, 2017.

793 Jacq, V., Ridame, C., L'Helguen, S., Kaczmar, F., and Saliot, A.: Response of the  
794 unicellular diazotrophic cyanobacterium *Crocospaera watsonii* to iron limitation,  
795 PLoS One, 9, e86749, 10.1371/journal.pone.0086749, 2014.

796 Jickells, T. D., An, Z. S., Andersen, K. K., Baker, A. R., Bergametti, G., Brooks, N., Cao,  
797 J. J., Boyd, P. W., Duce, R. A., Hunter, K. A., Kawahata, H., Kubilay, N., laRoche,  
798 J., Liss, P. S., Mahowald, N., Prospero, J. M., Ridgwell, A. J., Tegen, I., and Torres,  
799 R.: Global iron connections between desert dust, ocean biogeochemistry, and  
800 climate, Science, 308, 67-71, 10.1126/science.1105959, 2005.

801 [Karlusich, J. J. P., Pelletier, E., Lombard, F., Carsique, M., Dvorak, E., Colin, S., Picheral,](#)  
802 [M., Cornejo-Castillo, F. M., Acinas, S. G., Pepperkok, R., Karsenti, E., de Vargas,](#)  
803 [C., Wincker, P., Bowler, C., Foster, R. A.: Global distribution patterns of marine](#)  
804 [nitrogen-fixers by imaging and molecular methods, Nat. Commun., 12,](#)  
805 [10.1038/s41467-021-24299-y, 2021.](#)

806 Krupke, A., Mohr, W., LaRoche, J., Fuchs, B. M., Amann, R. I., and Kuypers, M. M.: The  
807 effect of nutrients on carbon and nitrogen fixation by the UCYN-A-haptophyte  
808 symbiosis, Isme J, 9, 1635-1647, 10.1038/ismej.2014.253, 2015.

809 [Kustka, A., Sañudo-Wilhelmy, S., Carpenter, E. J., Capone, D. G., and Raven, J. A.: A](#)  
810 [revised estimate of the iron use efficiency of nitrogen fixation, with special](#)  
811 [reference to the marine cyanobacterium \*Trichodesmium\* spp. \(cyanophyta\), J.](#)

812 [Phycol., 39, 12-25, 10.1046/j.1529-8817.2003.01156.x, 2003.](#)

813 Kupper, H., Setlik, I., Seibert, S., Prasil, O., Setlikova, E., Strittmatter, M., Levitan, O.,  
814 Lohscheider, J., Adamska, I., and Berman-Frank, I.: Iron limitation in the marine  
815 cyanobacterium *Trichodesmium* reveals new insights into regulation of  
816 photosynthesis and nitrogen fixation, *New Phytol.*, 179, 784-798, 10.1111/j.1469-  
817 8137.2008.02497.x, 2008.

818 Landolfi, A., Prowe, A. E. F., Pahlow, M., Somes, C. J., Chien, C. T., Schartau, M.,  
819 Koeve, W., and Oschlies, A.: Can top-down controls expand the ecological niche of  
820 marine N<sub>2</sub> fixers?, *Front Microbiol*, 12, 690200, 10.3389/fmicb.2021.690200, 2021.

821 Langlois, R. J., Hummer, D., and LaRoche, J.: Abundances and distributions of the  
822 dominant *nifH* phylotypes in the Northern Atlantic Ocean, *Appl. Environ.*  
823 *Microbiol.*, 74, 1922-1931, 10.1128/AEM.01720-07, 2008.

824 Langlois, R. J., Mills, M. M., Ridame, C., Croot, P., and LaRoche, J.: Diazotrophic  
825 bacteria respond to Saharan dust additions, *Mar. Ecol. Prog. Ser.*, 470, 1-14,  
826 10.3354/meps10109, 2012.

827 Le Borgne, R., Barber, R. T., Delcroix, T., Inoue, H. Y., Mackey, D. J., and Rodier, M.:  
828 Pacific warm pool and divergence: Temporal and zonal variations on the equator  
829 and their effects on the biological pump, *Deep Sea Research Part II*, 49, 2471-2512,  
830 10.1016/S0967-0645(02)00045-0, 2002.

831 Li, W., Sunda, W. G., Lin, W., Hong, H., and Shi, D.: The effect of cell size on cellular Zn

832 and Cd and Zn-Cd-CO<sub>2</sub> colimitation of growth rate in marine diatoms, *Limnol.*  
833 *Oceanogr.*, 65, 2896-2911, 10.1002/lno.11561, 2020.

834 Li, X., Wu, K., Gu, S., Jiang, P., Li, H., Liu, Z., and Dai, M.: Enhanced biodegradation of  
835 dissolved organic carbon in the western boundary Kuroshio Current when intruded  
836 to the marginal South China Sea, *J Geophys Res-Oceans*, 126, e2021JC017585,  
837 10.1029/2021jc017585, 2021.

838 Lu, Y., Wen, Z., Shi, D., Lin, W., Bonnet, S., Dai, M., and Kao, S. J.: Biogeography of N<sub>2</sub>  
839 fixation influenced by the western boundary current intrusion in the South China  
840 Sea, *J Geophys Res-Oceans*, 124, 6983-6996, 10.1029/2018jc014781, 2019.

841 [Ma, J., Yuan, D. X., Liang, Y., and Dai, M. H.: A modified analytical method for the](#)  
842 [shipboard determination of nanomolar concentrations of orthophosphate in](#)  
843 [seawater, \*J Oceanogr.\* 64, 443-449, 2008.](#)

844 Mohr, W., Großkopf, T., Wallace, D. W., and LaRoche, J.: Methodological  
845 underestimation of oceanic nitrogen fixation rates, *PLoS One*, 5, e12583,  
846 10.1371/journal.pone.0012583.g001, 2010.

847 Moisander, P. H., Beinart, R. A., Voss, M., and Zehr, J. P.: Diversity and abundance of  
848 diazotrophic microorganisms in the South China Sea during intermonsoon, *Isme J*,  
849 2, 954-967, 10.1038/ismej.2008.51, 2008.

850 Moisander, P. H., Zhang, R., Boyle, E. A., Hewson, I., Montoya, J. P., and Zehr, J. P.:  
851 Analogous nutrient limitations in unicellular diazotrophs and *Prochlorococcus* in



852 the South Pacific Ocean, *Isme J*, 6, 733-744, 10.1038/ismej.2011.152, 2012.

853 Montoya, J. P., Voss, M., Kähler, P., and Capone, D. G.: A simple, high-precision, high-  
854 sensitivity tracer assay for N<sub>2</sub> fixation, *Appl. Environ. Microbiol.*, 62, 986-993,  
855 10.1128/AEM.62.3.986-993.1996, 1996.

856 Needoba, J. A., Foster, R. A., Sakamoto, C., Zehr, J. P., and Johnson, K. S.: Nitrogen  
857 fixation by unicellular diazotrophic cyanobacteria in the temperate oligotrophic  
858 North Pacific Ocean, *Limnol. Oceanogr.*, 54, 1317–1327,  
859 10.4319/lo.2007.52.4.1317, 2007.

860 [Rodriguez, F., Lillington, J., Johnson, S., Timmel, C. R., Lea, S. M., and Berks, B. C.:](#)  
861 [Crystal structure of the bacillus subtilis phosphodiesterase PhoD reveals an iron and](#)  
862 [calcium-containing active site, \*J. Biol. Chem.\*, 289, 30889-30899,](#)  
863 [10.1074/jbc.M114.604892, 2014.](#)

864 Rubin, M., Berman-Frank, I., and Shaked, Y.: Dust- and mineral-iron utilization by the  
865 marine dinitrogen-fixer *Trichodesmium*, *Nat Geosci*, 4, 529-534,  
866 10.1038/ngeo1181, 2011.

867 Saito, M. A., Goepfert, T. J., and Ritt, J. T.: Some thoughts on the concept of colimitation:  
868 Three definitions and the importance of bioavailability, *Limnol. Oceanogr.*, 53, 276-  
869 290, 10.4319/lo.2008.53.1.0276, 2008.

870 Saito, M. A., Bertrand, E. M., Dutkiewicz, S., Bulygin, V. V., Moran, D. M., Monteiro, F.  
871 M., Follows, M. J., Valois, F. W., and Waterbury, J. B.: Iron conservation by

872 reduction of metalloenzyme inventories in the marine diazotroph *Crocospaera*  
873 *watsonii*, Proc. Natl. Acad. Sci. U.S.A., 108, 2184-2189,  
874 10.1073/pnas.1006943108, 2011.

875 Sañudo-Wilhelmy, S. A., Kustka, A. B., Gobler, C. J., Hutchins, D. A., Yang, M., Lwiza,  
876 K., Burns, J. A., Capone, D. G., Ravenk, J. A., and Carpenter, E. J.: Phosphorus  
877 limitation of nitrogen fixation by *Trichodesmium* in the central Atlantic Ocean,  
878 Nature, 411, 66-69, 10.1038/35075041, 2001.

879 [Sargent, E. C., Hitchcock, A., Johansson, S. A., Langlois, R., Moore, C. M., LaRoche, J.,](#)  
880 [Poulton, A. J., and Bibby, T. S.: Evidence for polyploidy in the globally important](#)  
881 [diazotroph \*Trichodesmium\*, FEMS Microbiol. Lett., 363, 10.1093/femsle/fnw244,](#)  
882 [2016.](#)

883 Schlosser, C., Klar, J. K., Wake, B. D., Snow, J. T., Honey, D. J., Woodward, E. M. S.,  
884 Lohan, M. C., Achterberg, E. P., and Moore, C. M.: Seasonal ITCZ migration  
885 dynamically controls the location of the (sub)tropical Atlantic biogeochemical  
886 divide, Proc. Natl. Acad. Sci. U.S.A., 111, 1438-1442, 10.1073/pnas.1318670111,  
887 2014.

888 Shiozaki, T., Kodama, T., and Furuya, K.: Large-scale impact of the island mass effect  
889 through nitrogen fixation in the western South Pacific Ocean, Geophys. Res. Lett.,  
890 41, 2907-2913, 10.1002/2014GL059835 2014a.

891 Shiozaki, T., Nagata, T., Ijichi, M., and Furuya, K.: Nitrogen fixation and the diazotroph

892 community in the temperate coastal region of the northwestern North Pacific,  
893 Biogeosciences, 12, 4751-4764, 10.5194/bg-12-4751-2015, 2015a.

894 Shiozaki, T., Chen, Y. L. L., Lin, Y. H., Taniuchi, Y., Sheu, D. S., Furuya, K., and Chen,  
895 H. Y.: Seasonal variations of unicellular diazotroph groups A and B, and  
896 *Trichodesmium* in the northern South China Sea and neighboring upstream  
897 Kuroshio Current, Cont. Shelf Res., 80, 20-31, 10.1016/j.csr.2014.02.015, 2014b.

898 Shiozaki, T., Furuya, K., Kodama, T., Kitajima, S., Takeda, S., Takemura, T., and Kanda,  
899 J.: New estimation of N<sub>2</sub> fixation in the western and central Pacific Ocean and its  
900 marginal seas, Global Biogeochem. Cycles, 24, GB1015, 10.1029/2009gb003620,  
901 2010.

902 Shiozaki, T., Takeda, S., Itoh, S., Kodama, T., Liu, X., Hashihama, F., and Furuya, K.:  
903 Why is *Trichodesmium* abundant in the Kuroshio?, Biogeosciences, 12, 6931-6943,  
904 10.5194/bg-12-6931-2015, 2015b.

905 Shiozaki, T., Bombar, D., Riemann, L., Hashihama, F., Takeda, S., Yamaguchi, T.,  
906 Ehama, M., Hamasaki, K., and Furuya, K.: Basin scale variability of active  
907 diazotrophs and nitrogen fixation in the North Pacific, from the tropics to the  
908 subarctic Bering Sea, Global Biogeochem. Cycles, 31, 996-1009  
909 10.1002/2017gb005681, 2017.

910 [Snow, J. T., Schlosser, C., Woodward, E. M., Mills, M., Achterberg, E. P., Mahaffey, C.,](#)  
911 [Bibby, T. S., and Moore, C. M.: Environmental controls on the biogeography of](#)

912 [diazotrophy and \*Trichodesmium\* in the Atlantic Ocean. \*Global Biogeochem. Cycles\*,](#)  
913 [29, 865-884, 10.1002/2015GB005090, 2015.](#)

914 Sohm, J. A., Webb, E. A., and Capone, D. G.: Emerging patterns of marine nitrogen  
915 fixation, *Nature reviews. Microbiology*, 9, 499-508, 10.1038/nrmicro2594, 2011.

916 Sperfeld, E., Raubenheimer, D., and Wacker, A.: Bridging factorial and gradient concepts  
917 of resource co-limitation: Towards a general framework applied to consumers, *Ecol.*  
918 *Lett.*, 19, 201-215, 10.1111/ele.12554, 2016.

919 Stenegren, M., Caputo, A., Berg, C., Bonnet, S., and Foster, R. A.: Distribution and  
920 drivers of symbiotic and free-living diazotrophic cyanobacteria in the western  
921 tropical South Pacific, *Biogeosciences*, 15, 1559-1578, 10.5194/bg-15-1559-2018,  
922 2018.

923 Tanita, I., Shiozaki, T., Kodama, T., Hashihama, F., Sato, M., Takahashi, K., and Furuya,  
924 K.: Regionally variable responses of nitrogen fixation to iron and phosphorus  
925 enrichment in the Pacific Ocean, *Journal of Geophysical Research: Biogeosciences*,  
926 126, e2021JG006542, 10.1029/2021jg006542, 2021.

927 Thompson, A. W., Carter, B. J., Turk-Kubo, K. A., Malfatti, F., Azam, F., and Zehr, J. P.:  
928 Genetic diversity of the unicellular nitrogen-fixing cyanobacteria UCYN-A and its  
929 prymnesiophyte host, *Environ. Microbiol.*, 16, 3238-3249, 10.1111/1462-  
930 2920.12490, 2014.

931 Turk-Kubo, K. A., Achilles, K. M., Serros, T. R., Ochiai, M., Montoya, J. P., and Zehr, J.

932 P.: Nitrogenase (*nifH*) gene expression in diazotrophic cyanobacteria in the Tropical  
933 North Atlantic in response to nutrient amendments, *Front Microbiol*, 3, 386,  
934 10.3389/fmicb.2012.00386, 2012.

935 Wang, W. L., Moore, J. K., Martiny, A. C., and Primeau, F. W.: Convergent estimates of  
936 marine nitrogen fixation, *Nature*, 566, 205-211, 10.1038/s41586-019-0911-2, 2019.

937 Ward, B. A., Dutkiewicz, S., Moore, C. M., and Follows, M. J.: Iron, phosphorus, and  
938 nitrogen supply ratios define the biogeography of nitrogen fixation, *Limnol.*  
939 *Oceanogr.*, 58, 2059-2075, 10.4319/lo.2013.58.6.2059, 2013.

940 Watkins-Brandt, K. S., Letelier, R. M., Spitz, Y. H., Church, M. J., Böttjer, D., and White,  
941 A. E.: Addition of inorganic or organic phosphorus enhances nitrogen and carbon  
942 fixation in the oligotrophic North Pacific, *Mar. Ecol. Prog. Ser.*, 432, 17-29,  
943 10.3354/meps09147, 2011.

944 [Welschmeyer, N. A.: Fluorometric analysis of chlorophyll-a in the presence of](#)  
945 [chlorophyll-B and pheopigments. \*Limnol. Oceanogr.\*, 39, 1985-1992, 1994.](#)

946 Wen, Z., Browning, T. J., Cai, Y., Dai, R., Zhang, R., Du, C., Jiang, R., Lin, W., Liu, X.,  
947 Cao, Z., Hong, H., Dai, M., and Shi, D.: Nutrient regulation of biological nitrogen  
948 fixation across the tropical western North Pacific, *Sci. Adv.*, 8, eabl7564,  
949 10.1126/sciadv.abl7564, 2022.

950 [White, A. E., Watkins-Brandt, K.S., and Church, M. J.: Temporal variability of](#)  
951 [Trichodesmium spp. and diatom-diazotroph assemblages in the North Pacific](#)

Deleted: Science Advances,

953 [Subtropical Gyre, Front. Mar. Sci., 5, 10.3389/fmars.2018.00027, 2018.](#)

954 Wu, C., Fu, F. X., Sun, J., Thangaraj, S., and Pujari, L.: Nitrogen fixation by

955 *Trichodesmium* and unicellular diazotrophs in the northern South China Sea and the

956 Kuroshio in summer, Sci Rep-Uk, 8, 2415, 10.1038/s41598-018-20743-0, 2018.

957 Wu, J., Chung, S. W., Wen, L. S., Liu, K. K., Chen, Y. L. L., Chen, H. Y., and Karl, D.

958 M.: Dissolved inorganic phosphorus, dissolved iron, and *Trichodesmium* in the

959 oligotrophic South China Sea, Global Biogeochem. Cycles, 17, 1008,

960 10.1029/2002gb001924, 2003.

961 Xu, M. N., Zhang, W., Zhu, Y., Liu, L., Zheng, Z., Wan, X. H. S., Qian, W., Dai, M., Gan,

962 J., Hutchins, D. A., and Kao, S. J.: Enhanced ammonia oxidation caused by lateral

963 Kuroshio intrusion in the boundary zone of the northern South China Sea, Geophys.

964 Res. Lett., 45, 6585-6593, 10.1029/2018gl077896, 2018.

965 [Yong, S. C., Roversi, P., Lillington, J., Rodriguez, F., Krehenbrink, M., Zeldin, O. B.,](#)

966 [Garman, E. F., Lea, S. M., and Berks, B. C.: A complex iron-calcium cofactor](#)

967 [catalyzing phosphotransfer chemistry, Science, 345, 1170-1173,](#)

968 [10.1126/science.1254237, 2014.](#)

969 Zehr, J. P. and Capone, D. G.: Changing perspectives in marine nitrogen fixation,

970 Science, 368, eaay9514, 10.1126/science.aay9514, 2020.

971 Zhang, J. Z.: [Shipboard automated determination of trace concentrations of nitrite and](#)

972 [nitrate in oligotrophic water by gas-segmented continuous flow analysis with a](#)

973 [liquid waveguide capillary flow cell, Deep Sea Research Part I, 47, 1157-1171,](#)  
974 [10.1016/S0967-0637\(99\)00085-0, 2000.](#)

975 Zhang, R., Zhu, X., Yang, C., Ye, L., Zhang, G., Ren, J. L., Wu, Y., Liu, S. M., Zhang, J.,  
976 and Zhou, M.: Distribution of dissolved iron in the Pearl River (Zhujiang) Estuary  
977 and the northern continental slope of the South China Sea, Deep Sea Research Part  
978 II, 167, 14-24, 10.1016/j.dsr2.2018.12.006, 2019.